ORIGINAL PAPER

CrossMark

The phase differences of the interdecadal variabilities of tropical cyclone activity in the peak and late seasons over the western North Pacific

Tingting Fan[1] · Shibin Xu[1] (iD) · Fei Huang[1,2] · Jinping Zhao[1,2]

© Springer-Verlag GmbH Austria, part of Springer Nature 2018

Abstract
This study compares the interdecadal variations in tropical cyclone (TC) activities over the western North Pacific (WNP) basin during the peak season (July–September) and late season (October–December) of 1955–2014 and explores the possible physical mechanisms behind the variations. Both the peak- and late-season tropical storm (TS) days show distinct interdecadal variations, while the late-season TS days lead the peak-season TS days by approximately 4 years on an interdecadal time scale. The late-season TC activity is related to the east-west sea surface temperature (SST) gradient across the equatorial Pacific. The westerly winds induced by the SST gradient can reduce the vertical wind shear and increase the low-level vorticity, which favors TC genesis over the TC genesis region. The peak-season TC activity appears to relate to the SST gradient between the Indian Ocean and the Central Pacific. The westerly wind induced by the SST gradient can reduce the vertical wind shear and increase the mid-level relative humidity, thereby enhancing the TC activity. The full picture of the interdecadal variation in the WNP TC activity during the peak and late seasons revealed in this study provides a new perspective on the seasonal TC forecasts and future projections.

1 Introduction

Tropical cyclones (TCs) are among the most severe natural disasters with respect to the loss of human life, property damage, and other economic consequences (Chan 2005). Approximately one third of the total global TCs are generated in the western North Pacific (WNP), and more frequent and intense TCs occur in this region than in any other ocean basins. In addition, TC activity may play a role in driving the ocean thermohaline circulation, thereby regulating the global climate (Emanuel 2001). Hence, many studies have focused on the historical changes and mechanisms of TC activity, which are helpful for TC activity forecasts and disaster reduction.

✉ Shibin Xu
xushibin@ouc.edu.cn

[1] Physical Oceanography Laboratory, Ocean University of China, Qingdao, China

[2] Qingdao National Laboratory of Marine Science and Technology, Qingdao, China

Numerous studies have demonstrated that TC activity has a significant interdecadal variation over the WNP. Two broad peaks of TC activity appear in the 1960s and the 1990s (Yumoto and Matsuura 2001; Matsuura et al. 2003; Chan 2008). The decadal variations in TC activity were mainly attributed to the decadal changes in the Central Pacific SST and the associated atmospheric thermal and dynamic conditions (Matsuura et al. 2003; Chan 2008; Liu and Chan 2013). Some very recent works focused on the late-season (October–December, OND) TC activities (Hsu et al. 2014; Zhao and Wang 2016). In particular, Hsu et al. (2014) observed an abrupt shift of the late-season TC activity in the mid-1990s that was caused by the La Niña-type SST anomaly. Interestingly, a significant decadal shift of the peak-season (JASO) WNP TC activity has been detected in the late 1990s (He et al. 2015). According to previous studies, although the distinct interdecadal variations can be identified both in the peak season and in the late season, there are remarkable differences between them and their associated environmental conditions, which means the interdecadal variations in TC activity have a remarkable seasonal dependence, implying different physical mechanisms behind the TC activities in the different seasons.

The purposes of the present study are to compare the interdecadal variability of the TC activity in the peak season

with that in the late season over the WNP, to illustrate the different characteristics of these variations, to examine how changes in oceanic and atmospheric conditions contribute to the TC activity in the desired seasons for a relatively long period, and to explore the associated physical mechanisms. The data sets and methods are given in "Section 2." Results are presented in "Section 3." A discussion and summary are provided in "Section 4."

2 Data and methods

The 6-hourly best track TC data over the WNP were obtained from the Joint Typhoon Warning Center (JTWC; https://metocph.nmci.navy.mil/jtwc/best_tracks/) for the period 1955–2014. In this study, we used tropical storm (TS) days to depict the TC activity during the peak season (from July to September, JAS) and the late season (from October to December, OND).

In addition to the TC datasets, several atmospheric and oceanic variables were used to examine large-scale environmental conditions: the monthly mean zonal and meridional wind components at the 850- and 200-hPa levels and the 700-hPa relative humidity from the twentieth century reanalysis dataset from the ECWMF (Poli et al. 2016) on a 1° × 1° grid in the years 1955–2010, as well as the monthly SST data from the Met Office Hadley Center Sea Ice and Sea Surface Temperature dataset version 1 (HadISST1; Rayner et al. 2003) on a 1° × 1° grid in the years 1955–2014.

To quantify the influence of the large-scale environmental factors on TC genesis number, we use the Genesis Potential Index (GPI; Emanuel and Nolan 2004) in this study. The GPI takes a set of environmental variables that include the potential intensity (Emanuel 1986), relative humidity, absolute vorticity, and vertical wind shear, and combines them into a single term. The vertical wind shear is defined as the magnitude of the vector difference between the horizontal winds at 200- and 850-hPa.

A data-adaptive method called the ensemble empirical mode decomposition (EEMD) method (Wu and Huang 2009) is performed in the present study to extract the low-frequency behaviors from the abovementioned variables.

3 Results

3.1 The interdecadal variations of the TS days

To explore the interdecadal variability of TC activity in the WNP basin, we extended our analysis back to 1955 and considered the peak season of July–September (JAS) and the late season of October–December (OND). Figure 1a shows the time series of the TS days over the WNP in JAS and OND for the period 1955–2014. After the EEMD method is applied,

both the TS days in the peak season and those in the late season show robust interdecadal variations over the years examined (Fig. 1a). The interdecadal variations in the TS days in the two seasons have similar cycles. It is interesting to note that there is a phase difference between the JAS TS days and the OND TS days. To confirm our findings, we computed the lagged cross-correlation of the JAS TS days with the OND TS days for the period 1955–2014 (Fig. 1b). Apparently, the most significant positive correlation is detected when the OND TS days lead the JAS TS days by approximately 4 years ($r = 0.81$). The cross-validation method (Michaelsen 1987) is performed to make a retrospective forecast (hindcast) for OND TS days by JAS TS days. The hindcast OND TS days is shown by the dotted line in Fig. 1a. The temporary correlation coefficient skill is 0.87 of the 55-year cross-validation, suggesting that the OND TS days may be considered as a predictor of JAS TS days on an interdecadal time scale. Furthermore, we checked their relationship during the period 1965–2014, when the observations of TS days are more reliable, the lead-lagged relationship will not be changed (Fig. S2).

Based on the time series of the interdecadal variations of TS days in JAS and OND, we identified two active periods (1961–1971 and 1989–1999) and two inactive periods (1975–1985 and 2008–2014). We computed the averages of the TS days, genesis numbers, and life spans for each period, as well as the differences in these three variables between the active and inactive periods in the corresponding season (Table 1). In the peak season, the average number of TS days is approximately 82.5 per year during the active periods and approximately 62.3 per year during the inactive periods; the epoch difference in the TS days is mainly caused by the reduction in the TC genesis number, and the mean life span did not show a statistically significant change. In the late season, the average number of TS days is 46.9 per year and 32.3 per year for the active and inactive periods, respectively. At the same time, the mean life span of the TCs is reduced from 6.4 to 5.4 days, showing a significant difference. Hence, the epoch difference in the TS days in OND is due to changes in both the TC genesis number and the mean life span.

Additionally, Fig. 2 shows the spatial distribution of the differences in the TC genesis numbers between active and inactive periods. For the peak season, positive TC genesis number differences can be found in most parts of the WNP basin; specifically, the significant values are mainly located in the region east of 130° E (Fig. 2a), indicating that there are more TCs over this region (10°–30° N, 130°–175° E) during the active periods. For the late season, significantly positive values are concentrated in the southeastern part of the WNP (5°–20° N, 135°–175° E), implying that the interdecadal changes of the late-season TC genesis numbers are mainly located in the southeastern part of the WNP (Fig. 2b), which is consistent with Matsuura et al. (2003). Furthermore, Wang and Chan (2002) suggested that the TCs with geneses in the
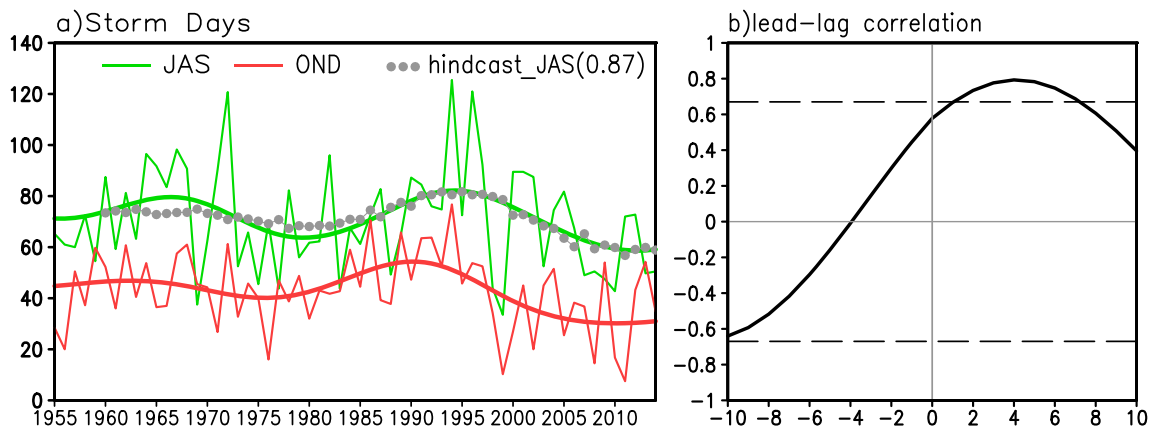
Fig. 1 **a** Time series of the TS days over the WNP basin for the period 1951–2014 (green and red indicate the peak season (JAS) and the late season (OND), respectively). Thin curves are based on the unsmoothed data, and thick curves are the decadal components of the TS days after EEMD is applied. The gray dotted line is hindcasted JAS TS days using the OND TS days. **b** The lead-lag correlation between the two thick curves (decadal components) is shown in **a**. The TC records are based on the best track data from JTWC

southeastern part of the WNP tend to have longer lifespans, which also induces more TS days (Fig. S1). Thus, the contributions from the genesis numbers and life spans are comparable to the TS days' changes (Table 1).

3.2 The interdecadal change in GPI

It is well known that the genesis of a tropical cyclone depends on large-scale atmospheric and oceanic conditions (Gray 1979) and that the GPI (Emanuel and Nolan 2004) can be used to quantify the influences of these conditions on TC genesis numbers. Here, we investigated the GPI to diagnose the interdecadal changes in TC genesis. During both JAS and OND, significantly positive GPI values consistently appeared over the positive TC genesis region (Fig. 2c,d), implying the interdecadal changes of GPI are consistent with the interdecadal changes of TC genesis numbers.

Additionally, we computed the area-averaged GPI changes and the contributions of each constituent term during JAS and OND over the TC genesis regions from the inactive periods to the active periods. By taking the logarithm in GPI formula, the

sum of the four constituent terms changes is identical to the total GPI changes (Table 2). Among the dynamic and thermodynamic factors, the vertical wind shear makes the largest contribution to the GPI changes in JAS and OND. The secondary contributor is the 700-hPa relative humidity (RH) in JAS and the 850-hPa vorticity (VOR) in OND. The MPI appears to be less important in the two seasons, which is consistent with that of Chan (2009) and suggests that local SSTs are not as important as the atmospheric conditions to TC genesis in the WNP.

Figure 3 shows the normalized time series of the interdecadal components in GPI and the two most dominant contributors in JAS and OND during 1955–2010. Notably, all records are based on the decadal components of the EMMD of each corresponding variable for the examined period. In JAS, the GPI, RH, and VWS records are all area-averaged over the region (10°–30° N, 130–175° E). During OND, the GPI, VWS, and VOR records are all averaged over the region (5°–20° N, 135–175° E). Note that the VWS record has been multiplied by − 1 to facilitate comparison with the other time series. All records show generally similar and physically

Table 1 Seasonal mean of the peak-season and late-season TS days, TC numbers and lifespans for the active (H) and inactive (L) periods, and their differences (H − L). The p values in italics indicate that the epochal change is statistically significant at the 5% level based on the nonparametric t test

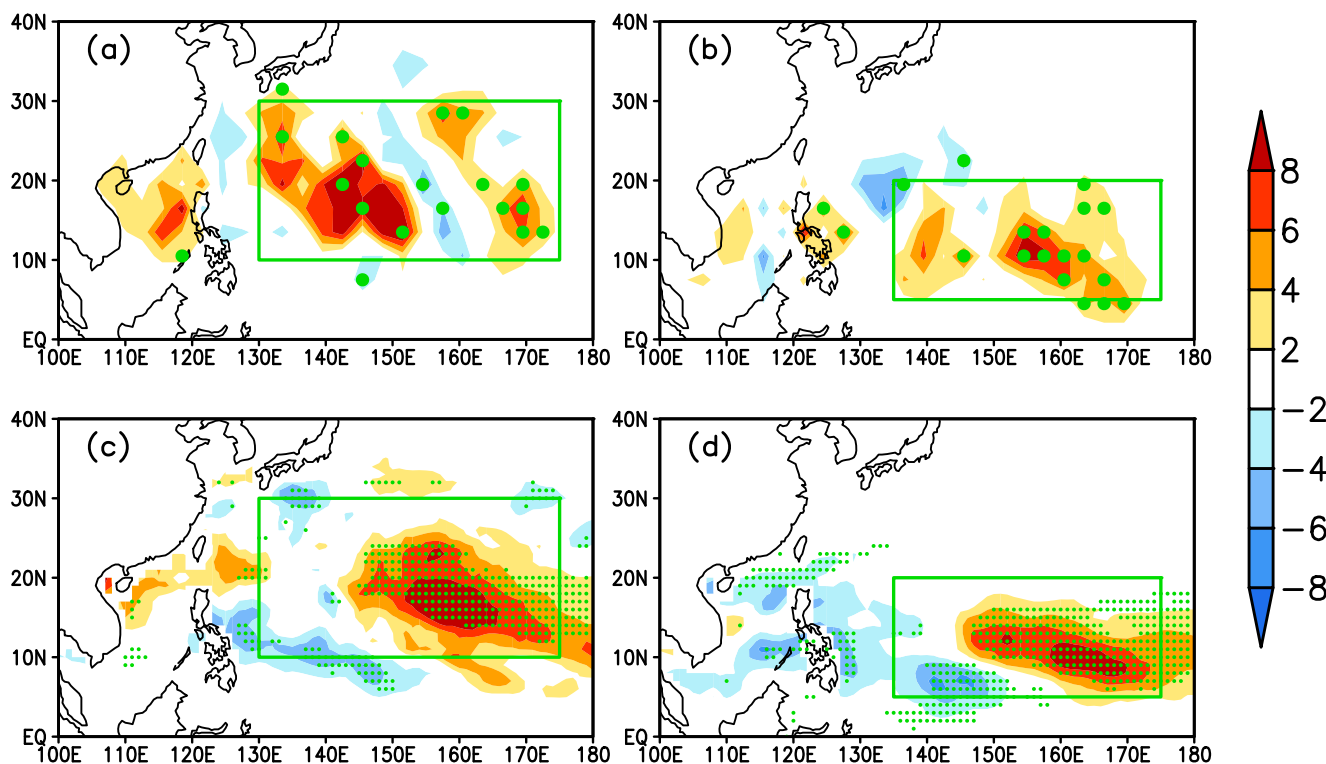|		TS days	TC number	Mean life span
Peak season	H (1961–1971, 1989–1999)	82.55	15.62	5.2
	L (1975–1985, 2008–2014)	62.31	12.7	4.9
	H − L	20.24	2.92	0.3
	p value	*0.001283*	*0.000233*	0.264155
Late season	H (1957–1967, 1985–1995)	46.965	7.85	6.4
	L (1971–1981, 2005–2014)	32.31	6.17	5.4
	H − L	14.66	1.67	1.0
	p value	*0.000206*	*0.002946*	*0.012192*

Fig. 2 Maps of the differences in the TC genesis numbers between the active and inactive periods in **a** JAS and in **b** OND. The green rectangular boxes in **a** and **b** indicate the regions with large differences. **c** and **d** are the same as in **a** and **b**, respectively, but for GPI. Green dots mark regions where the differences between the two periods are significant at the 5% confidence level based on the nonparametric *t* test. The green rectangles indicate the key regions of interdecadal changes in TC activities during JAS (10°–30° N, 130°–175° E) and OND (5°–20° N, 135°–175° E). The TC records are based on the best track data from JTWC. The GPI is based on the ERA twentieth century reanalysis and HadISST

consistent low-frequency behaviors over the same periods as the TS days in JAS and OND (shown in Fig. 1a), respectively.

3.3 The interdecadal changes in the environmental conditions

As mentioned above, the atmospheric circulation is important for TC activities on an interdecadal time scale, so we examined and compared how changes in the large-scale circulations contribute to the interdecadal variability of TC activity during JAS and OND. Figure 4 shows the regression map of the 850-hPa winds with respect to the decadal component of the TS days during JAS and OND for the entire study period. In JAS, in the peak season of TC activity, the regressions exhibit a

significant and robust band of westerly winds through the maritime continent to the Central Pacific (Fig. 4a). The anomalous westerly winds occurring at low levels over the tropical region indicate a weakening of the vertical wind shear over the southeastern part of the WNP, which is the most dominant factor in the TC activities at the interdecadal time scale. At the same time, the anomalous westerly winds over the maritime continent and the southwestern part of the WNP imply an enhanced summer monsoon circulation during the summer, which can improve the ascending movement and provide more water vapor to enhance the TC activity (Chen and Huang 2008; Wu et al. 2013). Meanwhile, in the late season (OND), the regression map also shows a robust and significant band of westerlies, but it is shifted to the southeast and extends

Table 2 Changes in the total GPI and each constituent term (i.e., low-level vorticity (VOR), maximum potential intensity (MPI), relative humidity (RH), and vertical wind shear (VWS)) between the active and inactive periods over the TC genesis regions ((10°–30° N, 130°–175° E) in JAS and (5°–20° N, 135°–175° E) in OND. The fractional contributions of each term to the total GPI changes are presented in parentheses

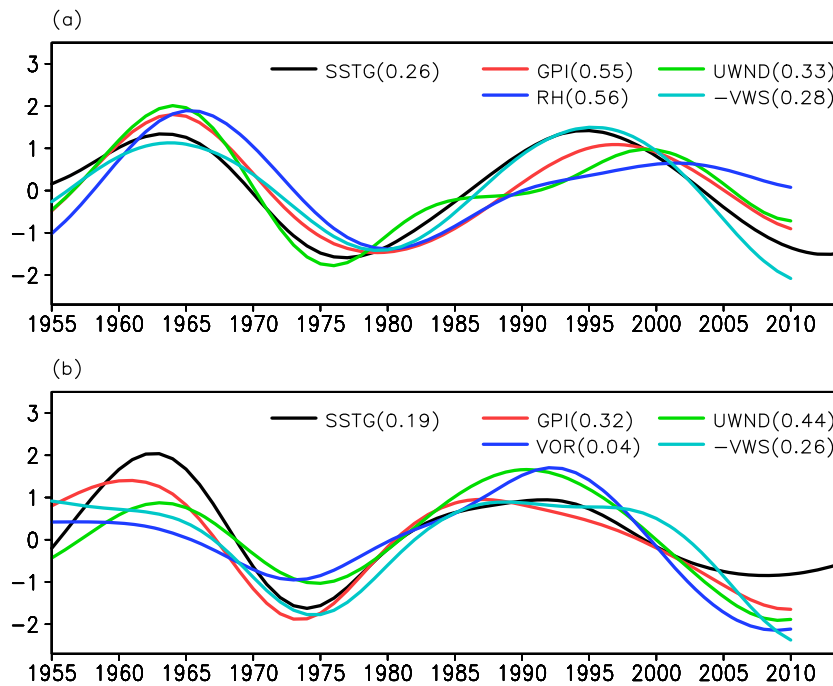|	GPI	VOR	MPI	RH	VWS
JAS	0.61 (100%)	0.09 (14%)	0.08 (13%)	0.18 (29%)	0.27 (44%)
OND	0.33 (100%)	0.11 (34%)	0.07 (22%)	−0.02 (−7%)	0.17 (52%)

Fig. 3 a Selected area-averaged time series in JAS during the period 1955–2010, shown as follows: SST difference between the Indian Ocean (35° S–10° N, 50–100° E) and the Central Pacific (10° S–10° N, 160° E–220° W), 850-hPa zonal wind (UWND; 10° S–10° N, 110°–170° E), GPI, 700-hPa relative humidity (RH) and vertical wind shear (VWS) over the region (10°–30° N, 130°–175° E). **b** Time series of the area-averaged SST differences between the Eastern Pacific (10° S–10° N, 170° W–130° W) and the Western Pacific (10° S–10° N, 110–150° E,), UWND (10°S–10° N, 150° E–150° W), GPI, VWS, and 850-hPa absolute vorticity (VOR) all over the region (5°–20° N,135–175° E). Note that all records are the decadal components of the EEMDs and are normalized by dividing by their standard deviations. The standard deviations are labeled in the legends. VWS is defined as the magnitude of the vector difference between the horizontal winds at 850 and 200 hPa

through the western Pacific to the eastern Pacific (Fig. 4b). The westerly winds over the southeastern part of the WNP induce weak vertical wind shear and enhance the low-level vorticity over the TC genesis region, which are the two dominant factors for the late-season GPI changes, and enhance the TC activity. The area-average zonal winds over the region (10° S–10° N, 110°–170° E) and the region (10° S–10° N, 150° E–150° W) in JAS and OND, respectively, are also shown in Fig. 3. The time series of zonal winds in the tropical regions are consistent with those of GPI, and they exhibit strong positive correlations ($r = 0.93$ and $r = 0.83$ for JAS and OND, respectively, Tab. S1).

To determine what caused the different locations of the westerly winds, we computed the regressions of the SST with respect to the decadal component of the area-averaged zonal wind in JAS and OND (shown in Fig. 4a,b, respectively). The regression map shows a positive center in the Central Pacific and a negative center in the Indian Ocean in JAS, indicating that the interdecadal component in zonal wind over the maritime continent and the western tropical Pacific is induced by the SST gradient between the Central Pacific and the Indian Ocean (Fig. 4a). In OND, the regression map shows an IPO-like pattern in OND, indicating that the interdecadal changes in zonal wind over the Central Pacific are mainly induced by the zonal SST gradient in the tropical Pacific (Fig. 4b).

We also computed the regressions of the velocity potentials and divergence winds at 850 hPa with respect to the decadal component of the TS days in JAS and OND (shown in Fig. 4c,d). In JAS, the divergence and convergence centers are located in the Indian Ocean and the Central Pacific, respectively. Thus, there is a robust westerly divergence wind over the maritime continent and the western tropical Pacific. During OND, the divergence center shifts to the maritime continent, and the convergence center shifts to the eastern tropical Pacific; thus, the robust westerly divergence wind shifts eastward. The convergence (divergence) centers are consistent with the cold (warm) centers in Fig. 4a,b, and confirmed that the westerly winds in tropical regions are determined by the SST boundary forcing.

Additionally, the SST gradients between the convergence centers and the divergence centers in JAS and OND are shown in Fig. 3. The interdecadal variations of the SST gradient show generally similar low-frequency behaviors to those of the zonal wind and the GPI in the corresponded season, with distinct seasonal features that are consistent with the regression maps discussed above. The interdecadal components of SST gradients also have significant correlations with the TS days in the corresponded seasons (Tab. S1).

Collectively, the overall agreement among these records, in terms of both their spatial patterns and their
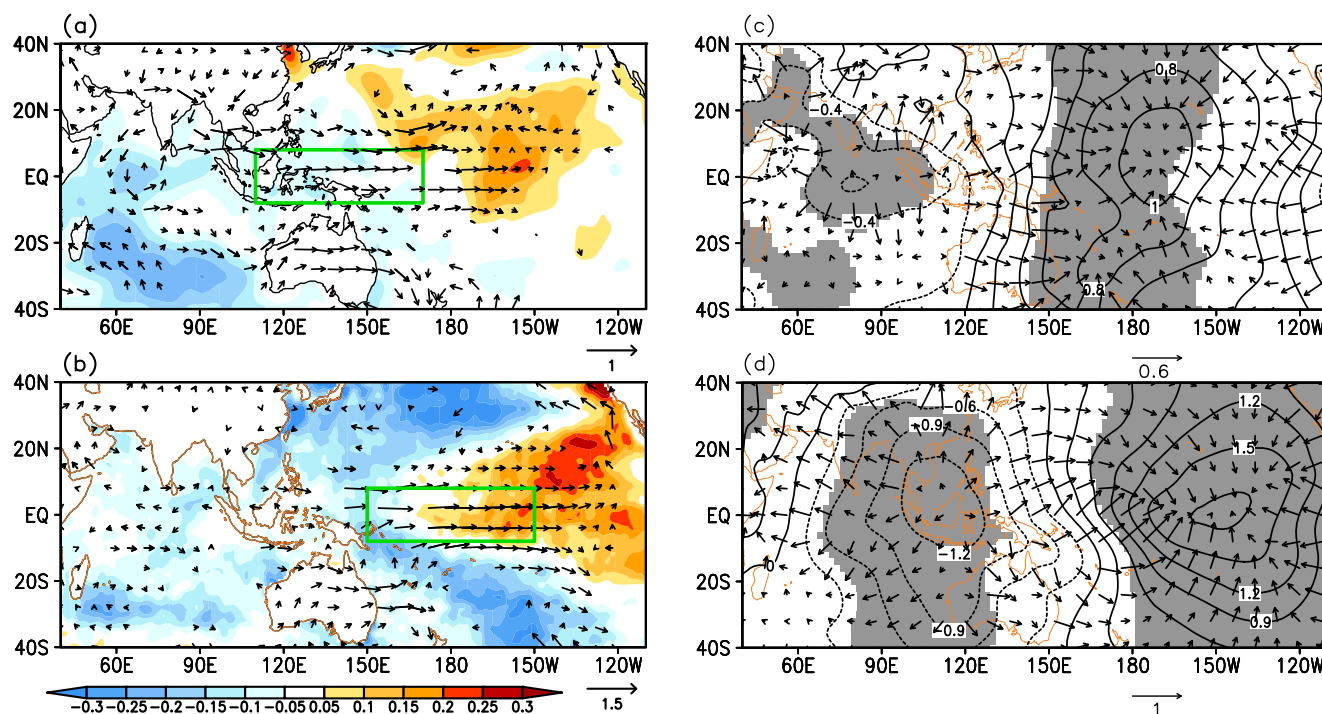
Fig. 4 **a** Spatial regression of the 850-hPa wind (vector,m/s) with respect to the interdecadal component of JAS TS days (only areas where the regression is significant at the 95% confidence level are shown), and spatial regression of the SST (shading, °C) with respect to the interdecadal component of the averaged zonal wind over the green rectangle region. **b**
same as in **a**, but for OND. **c** and **d** are spatial regression of the velocity potential (contour; m²/s) and divergent wind (vector; m/s) with respect to the interdecadal component of JAS TS days (gray shading marks the regions where the regressions are significant at the 5% confidence level)

temporal variability (Figs. 3 and 4), provide compelling and reasonable causes for the distinguished interdecadal variability of the TS days over the WNP in the two seasons for 1955–2014.

4 Summary and discussion

In this paper, we have compared the interdecadal variations in TC activity in the peak season (JAS) with that in the late season (OND) over the WNP using the JTWC best track data during the period 1955–2014 and further explored the associated mechanisms. The basin-wide TC activities in these two seasons show quite similar interdecadal changes but include a phase difference between them. According to the lead-lag correlation, the OND TC activity leads the JAS TC activity by approximately 4 years. The implication is that TC forecasts can be improved by considering the two seasons separately. To investigate the key factors affecting TC activities on the interdecadal time scale, GPI and its budget terms were investigated. The results suggest that the interdecadal variations in TC activity during the peak season are mainly due to the changes in mid-level relative humidity and vertical wind shear over the TC genesis region, whereas the vertical wind shear and the low-

level vorticity are the most important factors for the variations in the late-season TC activity on the interdecadal time scale. The peak season TC activity is associated with the anomalous westerly winds through the maritime continent to the western tropical Pacific, which may be induced by the anomalous SST gradient between the Indian Ocean and the Central Pacific. The late-season TC activity is associated with the anomalous westerly wind through the western tropical Pacific to the central tropical Pacific, which may be induced by the anomalous SST gradient between the eastern and western tropical Pacific.

The results verified that the large-scale SST distribution and atmospheric circulation changes are more important than the local SST at the interdecadal time scale. Furthermore, the influences of SST patterns and their associated atmospheric circulations on TC activity depend on the seasons.

As suggested by previous studies, the interdecadal changes in zonal SST gradients in the tropical Pacific are mainly determined by the Pacific Decadal Oscillation (PDO) or the Interdecadal Pacific Oscillation (IPO). Although the mechanisms of the PDO and IPO have not been explained, the heat conditions in the Pacific can affect the Indian Ocean heat content on the interdecadal time scale; thus, the Indian Ocean heat content lags behind that

of the Pacific (Lee et al. 2002; Cai et al. 2008; Dong and McPhaden 2016). The mechanisms of this lag also require further research.

References

Cai W, Sullivan A, Cowan T (2008) Shoaling of the off-equatorial South Indian Ocean thermocline: is it driven by anthropogenic forcing? Geophys Res Lett, 35(12)

Chan JCL (2005) Interannual and interdecadal variations of tropical cyclone activity over the western North Pacific. Meteorog Atmos Phys 89:143–152

Chan JCL (2008) Decadal variations of intense typhoon occurrence in the western North Pacific. In Proceedings of the Royal Society of London A: Mathematical, Physical and Engineering Sciences, 464(2089):249–272. The Royal Society

Chan JCL (2009) Thermodynamic control on the climate of intense tropical cyclones. Proc R Soc A 465:3011–3021

Chen G, Huang R (2008) Influence of monsoon over the warm pool on interannual variation on tropical cyclone activity over the western North Pacific. Adv Atmos Sci 25(2):319–328

Dong L, McPhaden MJ (2016) Interhemispheric SST gradient trends in the Indian Ocean prior to and during the recent global warming Hiatus. J Clim 29(24):9077–9095

Emanuel KA (1986) An air-sea interaction theory for tropical cyclones. Part I: steady-state maintenance. J Atmos Sci 43:585–604

Emanuel KA (2001) Contribution of tropical cyclones to meridional heat transport by the oceans. J Geophys Res 106:14771–14781

Emanuel KA, Nolan DS (2004) Tropical cyclone activity and the global climate system. In 26th Conference on Hurricanes and Tropical Meteorolgy, 240–141

Gray WM (1979) Hurricanes: their formation, structure, and likely role in the tropical circulation, In Meteorology over the tropical oceans. D. B. Shaw, Roy. Meteor Soc., 155–218

He H, Yang J, Gong D, Mao R, Wang Y, Gao M (2015) Decadal changes in tropical cyclone activity over the western North Pacific in the late 1990s. Clim Dyn 45:3317–3329

Hsu PC, Chu PS, Murakami H, Zhao X (2014) An abrupt decrease in the late-season typhoon activity over the western North Pacific. J Clim 27(11):4296–4312

Lee T, Fukumori I, Menemenlis D, Xing Z, Fu L (2002) Effects of the Indonesian throughflow on the Pacific and Indian Oceans. J Phys Oceanogr 32(5):1404–1429

Liu KS, Chan JCL (2013) Inactive period of western North Pacific tropical cyclone activity in 1998–2011. J Clim 26:2614–2630

Matsuura T, Yumoto M, Iizuka S (2003) A mechanism of interdecadal variability of tropical cyclone activity over the western North Pacific. Clim Dyn 21:105–117

Michaelsen J (1987) Cross-validation in statistical climate forecast models. J Clim Appl Meteor 26(11):1589–1600

Poli P et al (2016) ERA-20c: an atmospheric reanalysis of the twentieth century. J Clim 29:4083–4097. https://doi.org/10.1175/JCLI-D-15-0556.1

Rayner NA, Parker DE, Horton EB, Folland CK, Alexander LA, Rowell DP, Kent EA, Kaplan A (2003) Global analyses of sea surface temperature, sea ice, and night marine air temperature since the late nineteenth century. J Geophys Res 108(D14):4407

Wang B, Chan JCL (2002) How strong ENSO events affect tropical storm activity over the western North Pacific. J Clim 15(13):1643–1658

Wu Z, Huang NE (2009) Ensemble empirical mode decomposition: a noise-assisted data analysis method. Adv Adapt Data Anal 1(01):1–41

Wu L, Zong H, Liang J (2013) Observational analysis of tropical cyclone formation associated with monsoon gyres. J Atmos Sci 70(4):1023–1034

Yumoto M, Matsuura T (2001) Interdecadal variability of tropical cyclone activity in the western North Pacific. J Meteorol Soc Jpn 79:23–35

Zhao H, Wang CZ (2016) Interdecadal modulation on the relationship between ENSO and typhoon activity during the late season in the western North Pacific. Clim Dyn 47:315–328